Efficient injection of gas tracers into rivers: A tool to study Surface water–Groundwater interactions

Water Research 254 (2024) 121375

Contents lists available at ScienceDirect

Water Research

journal homepage: www.elsevier.com/locate/watres

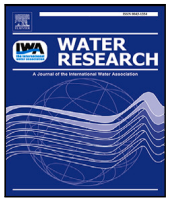

Efficient injection of gas tracers into rivers: A tool to study Surface water–Groundwater interactions

Théo Blanc [a,b,*], Morgan Peel [a], Matthias S. Brennwald [b], Rolf Kipfer [b,c], Philip Brunner [a]

[a] Centre for Hydrogeology and Geothermics of University of Neuchâtel (CHYN), Hydrochemistry and Contaminants and Hydrogeological processes, Rue Emile-Argand 11, Neuchâtel, 2000, Neuchâtel, Switzerland

[b] Eawag, Swiss Federal Institute of Aquatic Science and Technology, Water Resources and Drinking Water, Ueberlandstrasse 133, Dübendorf, 8600, Zürich, Switzerland

[c] Institute of Biogeochemistry and Pollutant Dynamics and Institute of Geochemistry and Petrology, Swiss Federal Institute of Technology (ETH), Universitätstrasse 16, Zürich, 8092, Zürich, Switzerland

ARTICLE INFO

Keywords:
Bank filtration
Diffusive injection
Noble gas
Infiltration
Stream

ABSTRACT

Surface water (SW) - groundwater (GW) interactions exhibit complex spatial and temporal patterns often studied using tracers. However, most natural and artificial tracers have limitations in studying SW–GW interactions, particularly if no significant contrasts in concentrations between SW and GW exist or can be maintained for long durations. In such context, (noble) gases have emerged as promising alternatives to add to the available tracer methods, especially with the recent development of portable mass spectrometers, which enable continuous monitoring of dissolved gas concentrations directly in the field. However, long-duration gas injection into river water presents logistical challenges. To overcome this limitation, we present an efficient and robust diffusion-injection apparatus for labeling large amounts of river water. Our setup allows fine, real-time control of the gas injection rate, and is suitable for extended injection durations and different gas species. To illustrate the effectiveness of our approach, we present a case study where helium (He) is used as an artificial tracer to study river water infiltration into an alluvial aquifer. Our injection of He as a tracer increased the dissolved He concentration of the river water by one order of magnitude compared to air-saturated water concentration for 35 days. This experiment yields valuable information on travel times from the river to a pumping well and on the mixing ratios between freshly infiltrated river water and regional groundwater.

1. Introduction

A better understanding of surface water–groundwater interactions (SGIs) is of primary importance to address numerous contemporary challenges affecting stream ecology, river management, agriculture, and the provision of sufficient quantities of high-quality drinking water to the human population (Barthel and Banzhaf, 2016; Boano et al., 2014; Brunner et al., 2017; Poff and Zimmerman, 2010).

Complex spatial and temporal patterns of SGIs limit the characterization of exchange fluxes and transit times of water infiltrating from surface water bodies to a specific location in the aquifer (e.g a drinking water well). Methods relying on tracers (either environmental or artificial) are commonly employed to overcome these challenges. In general, time-series of tracer concentrations in surface water (SW) and groundwater (GW) are collected and compared. These methods require significant differences in tracer concentrations between the two water bodies, or that temporal variations in SW concentrations can be clearly linked to those in GW (Brunner et al., 2017).

The injection of artificial tracers into SW bodies and monitoring of their concentrations in observation wells can allow identification of zones of SW infiltration. Tracers such as fluorescent dyes (e.g. fluorescein, sulforhodamine-B, etc..) or salts (e.g. bromide, iodide) have been used to this end (e.g. Davis et al., 1980; Lin et al., 2003). These methods are best suited to short injection times and in low-discharge rivers, as the amount of required tracer may otherwise quickly become financially and logistically prohibitive. Other practical considerations limit the use of fluorescent dyes in the field, as special authorizations and careful handling are required. Finally, coloring of river water (and possibly GW) for days or weeks might cause issues with public acceptance.

Environmental tracers like electrical conductivity (EC), temperature, or stable water isotopes ($d^{18}O$, $d^{2}H$) tend to be more widely

* Corresponding author at: Centre for Hydrogeology and Geothermics of University of Neuchâtel (CHYN), Hydrochemistry and Contaminants and Hydrogeological processes, Rue Emile-Argand 11, Neuchâtel, 2000, Neuchâtel, Switzerland.
E-mail address: theo.blanc@unine.ch (T. Blanc).

https://doi.org/10.1016/j.watres.2024.121375
Received 25 October 2023; Received in revised form 14 February 2024; Accepted 23 February 2024
Available online 24 February 2024

used than artificial tracers to study river infiltration into alluvial aquifers (Anderson, 2005; Cirpka et al., 2007; Coplen et al., 2000; Hoehn and Von Gunten, 1989; Stute et al., 1997), but in many cases provide only limited quantitative insight into SGIs. EC for example may not always be considered a conservative tracer, and measured values in SW may not vary sufficiently to be tied to variations in GW. Temperature is another non-conservative tracer, which may yield ambiguous results if the thermal parameters of the SW–GW interface and aquifer are not well-constrained (Schilling et al., 2019). Isotope methods may only be sensitive to processes at restricted timescales (e.g days for Radon-222 (Cecil and Green, 2000), or years for $^3H/^3He$ (Kipfer et al., 2002)) or their use limited by technical considerations (e.g. complicated sampling or measurement procedures, costs, etc...).

There is a need for novel tracer methods to enhance the understanding of SGIs (Schilling et al., 2019; Brunner et al., 2017). This is especially the case in the context of river-water infiltration in cases where sufficient contrasts in tracer concentrations between SW and GW do not exist or cannot be induced. Gases, and especially noble gases, present great potential for studying SGIs both as artificial or environmental tracers (see references in next paragraph). They offer several advantages over many existing methods, as they are invisible, odorless, and as most of them are non-toxic and readily available (Brennwald et al., 2022). Moreover, large volumes of compressed gas may be easily transported and handled in the field, and used in circumstances where the required amount of other artificial tracers would be impractical, e.g. in high-discharge rivers or for long injection times.

The recent development of portable on-site mass spectrometer measurement technology (Brennwald et al., 2016; Chatton et al., 2017; Mächler et al., 2012) has enhanced the potential of (noble) gases as tracers by allowing real-time and high-resolution quantification of dissolved gas concentrations (e.g. He, Kr and Xe (Brennwald et al., 2022)). This technology has recently been used for the study of SW–GW dynamics. For example, Mächler et al. (2012) used it to investigate SGIs in the hyporheic zone. More recently it has been used to study river water infiltration by monitoring natural variations in dissolved helium concentrations in observation wells (Popp et al., 2021), but some results were ambiguous owing to the low concentration gradients between river water and GW, as well as the unresolved mixing of different GW components in the pumping wells. Finally, SW–GW interactions were studied in Brennwald et al. (2022) by using several noble gases as artificial tracers in repeated pulse tracer tests in GW during a riverbed excavation experiment.

Injection of gas into rivers is a common method in hydrology to measure the gas transfer velocity, and therefore the reaeration rate of a river, or to study hyporheic exchange (Benson et al., 2014; Cirpka et al., 1993; Cook et al., 2006; Hall Jr. and Madinger, 2018; Knapp et al., 2019; Vautier et al., 2020; Lamontagne and Cook, 2007). It has hardly ever been conducted to study river infiltration into GW, likely owing to the experimental constraints of gas injection in high-energy environments over long periods of time (several weeks to several months). Indeed, the two existing methods, bubbling or diffusive injection, are respectively inefficient or permit only low injection rates.

Bubbling injection is usually carried out by placing perforated tubing or diffusion stones in water, and feeding gas from a tank to create numerous small bubbles, which will partially dissolve in water before reaching the surface (Clark et al., 2005; Knapp et al., 2015). The bubbling injection can also take place in a recipient, wherein a volume of water is loaded, and subsequently, the enriched water is directly injected into a water body. However, the injection of enriched water usually takes place directly into GW (Davis et al., 1985; Chatton et al., 2017; Brennwald et al., 2022). Although high supersaturation of dissolved gas concentration can be achieved with this method, most of the injected gas (95–99.5%) is typically lost to the atmosphere, which renders the quantification of the injected gas into water difficult (Benson et al., 2014; Clark, 2020).

In the case of diffusive injection, a similar setup is used, but the perforated tubing is replaced with a semi-permeable membrane (e.g. silicone rubber). This gas-permeable membrane enables gases to diffuse from the gas phase directly into water. This second method is much more efficient as it creates no bubbles and almost all the injected gas (99.9%–100%) dissolves into water (Benson et al., 2014; Clark, 2020). One caveat of this injection method is that only low injection rates (e.g. 2–3 $\cdot 10^{-5}$ mol/min) are generally achieved, which limit its use to rivers with low discharge (less than 1 m^3/s) (Benson et al., 2014; Cook et al., 2006; Knapp et al., 2019). Clark (2020) conducted two injection experiments using both methods to study river infiltration and to validate numerical flow model. They identified the spiked gas in the groundwater after the bubbling, but not after the diffusive injection.

There is, therefore, the need to develop a system for quantitative injection of large volumes of gases into rivers, that 1. is efficient, 2. allows control of the gas injection rate, and 3. allows precise quantification of gas injection rates into GW. In this work, we present a robust and effective diffusive injection technique that achieves these goals, and provide an example of its application to study river infiltration using the noble gas helium.

2. Development of our injection system

The diffusive gas transfer rate I_i [L^3 T^{-1}] of a gas species i across a semipermeable membrane is related to the membrane permeability k_i [L^3 M^{-1} T] to the gas species i, the partial gas pressure difference across the membrane ΔP_i [M L^{-1} T^{-2}], the membrane thickness e [L], and the diffusive surface S [L^2] (Daynes, 1920):

$$I_i = k_i S \frac{\Delta P_i}{e} \quad (1)$$

An efficient gas injection scheme should therefore aim to maximize the diffusive area, and minimize the membrane thickness without compromising its integrity through high gas pressure gradients. A highly effective diffusive area can be achieved through the use of low-diameter tubing, i.e. with a high surface/volume ratio. Our diffusive injection setup was assembled using 100m-long sections of 4 × 6 mm inner and outer diameter (ID × OD) silicone tubing, i.e. with a wall thickness of 1 mm. 100-m sections of tubing were coiled around a concentric arrangement of 1- and 2-inch screened HDPE tubes, each approximately 2 meters in length. Third of the tubing was coiled around the 1-inch tube, while the remaining length was wound around the 2-inch tube, enabling water circulation through the screening (see Fig. 1). This arrangement allowed us to construct a compact diffusion cell, with a total diffusive inner area of approximately 1.9 m^2 per cell). One end of the silicone tubing was connected to a section of copper tubing (6 mm OD, 1 mm thickness), while the other was sealed with a hermetic cap. The copper tubing was used to connect the immersed silicone tubing to the gas tank. We selected copper tubing because its impermeability prevents the direct diffusion of gas into the atmosphere. Copper tubing can also withstand high pressure and remains easily bendable to adapt to different environment and situations. Finally, the coiled tubes were placed in a 3-inch screened PVC casing to mechanically protect the silicone tubing from objects transported by the river (e.g. tree branches, rocks, etc...). Both ends of the 3-inch casing were closed with plastic caps, one of which was drilled to place the copper tube.

The permeability of the selected silicone rubber to a gas can be estimated with Eq. (1) by controlled pressurization of the injection cells with the gas and monitoring the pressure decrease over time. We estimated the permeability for Helium (He) before starting our experiment. Estimated permeability k_{He} of the tubing to helium was on the order of 0.01 $cm^2/(s \cdot bar)$ at STP, leading, for each diffusion cell, to an injection rate I_{He} of about 0.2 ccSTP/s (i.e. approximately 53 $\cdot 10^{-5}$ mol/min) of helium per bar of overpressure (ΔP_i, STP stands in this paper for Standard Temperature (T) and Pressure (P), T = 273.15 K, P = 1 bar). Finally, the silicone tubing could be pressurized up to four

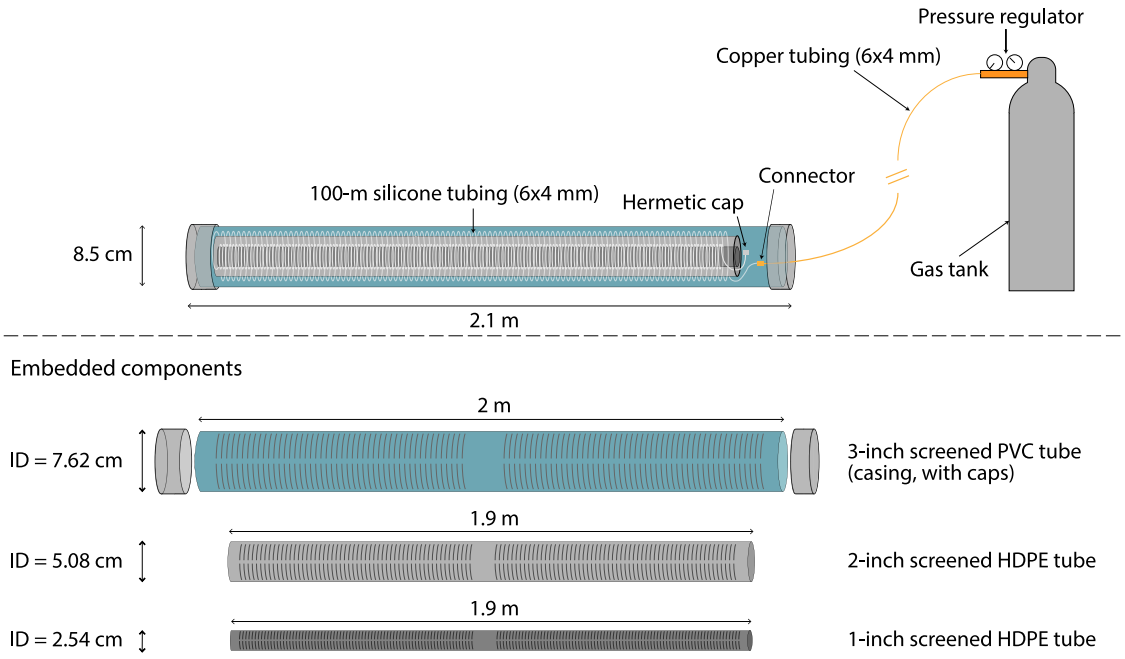

Fig. 1. Scheme of the diffusive injection setup. The silicone tubing and its connection with the copper tubing are placed within the 3-inch casing. The copper tubing connects the protective casing to the tracer gas tanks. ID: inner diameter.

bar without significant deformation. These numbers are indicative and can vary depending on the type of silicone used.

The presented setup is simple to assemble and consists of widely available components, with a cost of approximately 100 Swiss Francs per injection cell.[1] Furthermore, it is suitable for a range of tracer gases, with which the silicone tube has a higher permeability than that observed with helium. In the next section, we present a case study showing how we used our injection cells with three gas tanks of the noble gas helium.

3. Application of our system

The injection setup was tested in a pre-alpine valley river (Emme river) in central Switzerland (canton of Bern). At this location, the valley floor forms an alluvial aquifer used for drinking water production (Käser and Hunkeler, 2016; Popp et al., 2021; Schilling et al., 2017). The goal of our experiment was to study river infiltration using He as an artificial tracer. The location was selected because 1. it is highly monitored, and 2. uncertainties remained about the origin of the pumped groundwater and SW–GW mixing ratios, although previous studies suspected active and ongoing bank filtration (Schilling et al., 2017; Popp et al., 2021). Fig. 2 shows a map of the field site with a high productive drinking water well (3700 l/min), 6 piezometers (P1–P6) used in our studies, and the gas injection (IS) and measurement (MS, M1 and M2) locations. The production well is 10 meters deep, and the piezometers range in depth from 6 to 10 m. Based on a conceptual understanding of the field site coupled to the numerical model from Schilling et al. (2017), we suspected the infiltration zone, i.e. the location where the river water enters the groundwater body, to lie between the injection station (IS) and piezometer P3.

We used He as a gas tracer during our experiment, as this gas is inert, non-toxic, readily available, and relatively cheap compared to other noble gases. We aimed to increase He concentration in the river by at least 1 order of magnitude above He concentration of air saturated water (ASW). Thus, we used this targeted increase of He concentration, as well as the average discharge of the river (2–3 m^3/s), and the measured injection rate across the silicone tubing (0.2 ccSTP/s per bar of over-pressure and per injection cell) as a basis to estimate the number of cells required. We estimated to need eight diffusion cells as shown in Fig. 1, which represents 800 meters of 6 mm (OD) silicone tubing, i.e a total diffusive area of approximately 15 m^2. We tied the diffusion cells in pairs and placed them at the injection location of our field site (see "IS" in Fig. 2). They were attached to iron rods rammed into the riverbed and placed perpendicular to the flow direction, at a location constantly submerged by river water (i.e. avoiding the shallow sides of the river, see Fig. 3). Depending on discharge, the river width at the injection location was approximately 10–15 m. We could not place the injection cells over the entire width of the river, because the shape of the riverbed caused the current to be too strong in the center and the water to be too shallow on the edges of the river. We connected the cells to three 30-liter He gas tanks at 200 bar (i.e. containing a total volume of 18 m^3STP of He) stored on the riverbank; one of the tanks was connected to two pairs of diffusion cells, two others were connected to the two remaining injection cells. The three He gas tanks cost approximately 1000 Swiss Francs (price January 2021). The manual pressure regulators allowed to precisely control the gas pressure within the silicone tubing, and thus to control the gas injection rate. Although the silicone tubing can accommodate up to 4.5 relative bar of gas pressure (see Section 2), pressures were kept at maximum 3 bar (relative pressure) for the duration of the experiment.

The experiment started on February 6th, 2021 (day 0 in the figures). The first 6 days, we measured the SW and GW background concentrations (phase 0). Then, the gas was continuously injected into the stream for 35 days (from day 6 to 41). The He injection was separated in four phases (1 to 4), at 1.5 or 3 bar injection pressures, to induce a transient He signal in groundwater (see Table 1). These injection pressures correspond to a gas injection rate of approximately 2.5 and 5 ccSTP/s respectively. The silicone tubing of one cell was punctured on day 25, which led to only seven injection cells being operational in phase 3 and 4. In total, the 35-day injection phase only required the equivalent of He stored in the three tanks (approximately 18 m^3STP).

[1] Silicone tubing costs less than half a Swiss Franc per meter in length, and HDPE and PVC screened tubing costs between 10 and 20 Swiss Francs per piece. In total, an injection unit (cell and copper tubing) costs approximately 100 Swiss Francs (excluding gas tanks).

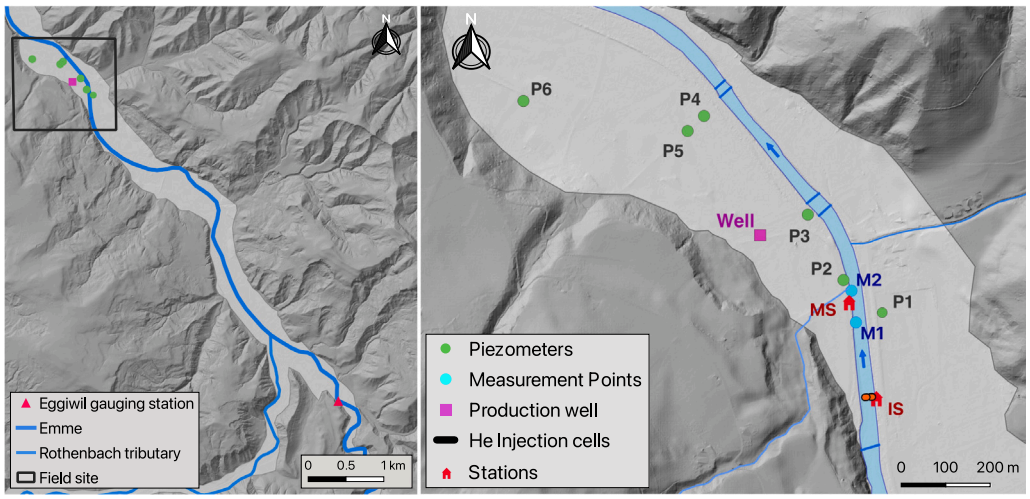

Fig. 2. Left: Location of our field site in the pre-alpine valley. This map also shows the gauging station of the Emme and the Röthenbach tributary. **Right:** Map of the alluvial plain at our field site. IS and MS stand for injection station and measurement station respectively. There is a miniRUEDI in both the production well and in the measurement station. The blue cross sections in the river indicate weirs, approximately 1 meter in height. (For interpretation of the references to color in this figure legend, the reader is referred to the web version of this article.)
Source: Maps modified from Swisstopo (2021).

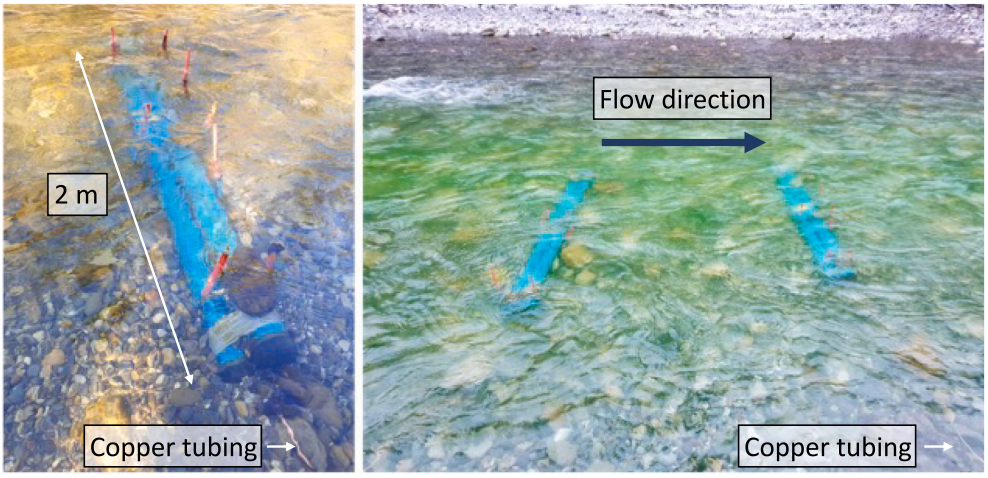

Fig. 3. Left: One pair of injection cells fixed on the riverbed. **Right:** Two pairs of injection cells fixed in the river. Note the copper tubing, which allows to feed the He to the diffusion cells, at the bottom right corners of both pictures.

Table 1
Information about the injection phases. We gradually increased the injection pressure during the 1st phase to test our setup and regularly checked for leaks.

Phase	Injection pressure [bar]	Start–End [day]	Number of cells used
0	0	0–6	0
1	1.5–2	6–11	8
2	3	11–27	8, (last 2 days 7)
3	1.5	27–34	7
4	3	34–41	7

3.1. Monitoring of dissolved gas concentrations

We used two portable gas-equilibrium membrane-inlet mass spectrometers (GE-MIMS) (miniRUEDI, Gasometrix GmbH, Switzerland (Brennwald et al., 2016)), to monitor dissolved gas concentrations continuously both in the river and in the pumping well.

We monitored the dissolved gases concentrations in the river at location M1 (see map on Fig. 2) for the duration of the experiment, at a time resolution of approximately six measurements per gases per hour. M1 was intentionally located 200 meters downstream of the injection station (IS) to let the injected He get mixed laterally and vertically, i.e. to get more representative measurements. We continuously monitored He, but also O_2, N_2, and Ar. To pump the river water, we used membrane pumps ("Minipuppy" and "Waterpuppy" pumps, Jabsco, Xylem Water Solutions UK Ltd.), because they can be kept outside of the river, avoiding damages caused by material transported in the river. We set the pumping hose entry approximately 20 cm above the riverbed to ensure pumping could occur even at very low river discharge rates and to reduce the risk of pump damage from fine sediment. The pumped river water flowed through a membrane module connected to one inlet of the miniRUEDI. The membrane module contains a small gas headspace which is in equilibrium with the flowing water according to Henry's law and this gas is then analyzed by the miniRUEDI. A sealed bag (Calibrated Instruments, Inc.) containing atmospheric ambient air was connected to another inlet of the miniRUEDI. This air was used as a calibration standard throughout the experiment. We attempted to discern potential degassing of excess dissolved He in the river by monitoring He concentration for one week at a second location in the river (M2), approximately 70 meters downstream of M1 (see Fig. 2). To achieve this, we used a second membrane pump that supplied water through another membrane module. This formed a separate water

circuit that was also connected to the miniRUEDI, via one of its multiple inlets.

The second miniRUEDI, at the production well, was used for the monitoring of the dissolved gas concentrations in the pumped groundwater. The same gases were analyzed as in the river, at similar time intervals. We collected water with a submersible pump.

Finally, we used the river miniRUEDI nine times to measure dissolved gas concentrations in six piezometers (see Fig. 2). We conducted these nine surveys at regular intervals from February to August 2021, to monitor the spatial and temporal evolution of dissolved gas concentration in the alluvial aquifer and to detect zones influenced by river water infiltration.

The piezometers and the production well all have very similar depths (between 6 and 10 m). Therefore, we assume that we mostly measured the dissolved gas concentrations of the groundwater from the upper part of the aquifer, characterized by an average thickness of 25 m and a maximum depth of 46 m (Würsten, 1991). As this aquifer shows mostly horizontal flow (Käser and Hunkeler, 2016), we expect the infiltrating He-enriched river water to be mostly present in this upper layer.

3.2. Estimation of the efficiency of the injection

We can calculate the efficiency ϵ [-] of the injection system in the river by comparing the measured dissolved He concentrations $C_{\mathrm{He,meas}}$ [ccSTP·g^{-1}] in the river at M1 (monitored by the miniRUEDI) to the theoretical He concentrations in the river $C_{\mathrm{He,calc}}$ [ccSTP·g^{-1}] assuming complete dissolution of injected He:

$$\epsilon = \frac{C_{\mathrm{He,meas}}}{C_{\mathrm{He,calc}}} \tag{2}$$

The theoretical He concentrations in river water $C_{\mathrm{He,calc}}$ are calculated with the He injection rate $I_{\mathrm{He,tot}}$ (0.2 ccSTP/s, multiplied by the gauge pressure and the number of injection cells), and with the Emme river discharge at the injection point Q_{Emme} [g·s^{-1}]:

$$C_{\mathrm{He,calc}} = \frac{I_{\mathrm{He,tot}}}{Q_{\mathrm{Emme}}} \tag{3}$$

Finally, we can get the total volume of gas injected by diffusion by integrating $I_{\mathrm{He,tot}}$ over the duration of the experiment. Comparing this volume with the total amount of He used in the experiment (i.e. the volume that left the gas tanks) allows the identification and quantification of the leaking volume.

3.3. Results

3.3.1. Concentration in the river

Fig. 4 shows the measured dissolved He concentrations of river water during the experiment, highlighting the four injection phases (Table 1) as well as the discharge of the Emme (Eggiwil gauging station, FOEN, 2018). River discharge at the gauging station was quite variable during our experiment (between 0.9 and 28 m^3/s), with an average flow of 3 m^3/s. This discharge is approximately 30% lower than at our field site, owing to the confluence of the Emme river with a tributary (Röthenbach river) between the gauging station and the study site (see Fig. 2).

The diffusive injection through silicone tubing resulted in, on average, He supersaturation in the river one order of magnitude above that of ASW, with concentrations varying between 5 to 24 times ASW concentration. This variation was mainly influenced by the discharge of the Emme. As the experiment took place towards the end of the winter season, diurnal fluctuations occurred in response of the snow melt during the day. The strong decrease in river He at the end of injection phases 2 and 4 are caused by the abrupt change of He pressure inside the injection cells (see Table 1). The decrease of concentration after one cell got punctured is visible on day 25 (the same day when we changed the pumps). For the nine-day period where He concentrations were simultaneously monitored at locations M1 and M2 (between days 25 and 34), there was an average decrease between both points of 10%–15%. This means that a small but significant fraction of dissolved He is degassed to the atmosphere between these two locations. However, this difference is small enough to assume that the river remains supersaturated in He while flowing on the suspected infiltration area, i.e between the injection location to the piezometer P3 (see Fig. 2). During the entire experiment, the concentrations of other dissolved gases (O_2, N_2 and Ar) remained stable at ASW concentrations, confirming that the observed He supersaturation is caused by our injection (see additional material in Appendix A).

There are some significant data gaps over the course of the experiment. The first measurement interruption occurred only a few hours after the start of the He injection, as the river intake pump froze because of a mean air temperature of −9 degrees (MeteoSwiss, 2021). We replaced the pump on day 13. However, the newly installed pump suffered from priming issues, leading to contamination of the water line with atmospheric air, making measurements unstable. Our measurements stabilized with the installation of a more powerful pump on day 25. On that same day, we also started to monitor dissolved He concentrations downstream, at M2. Therefore, we continuously measured dissolved He concentrations of river water from day 13 to day 34. Then, a high flow event (peak discharge 28 m^3/s at the Eggiwil gauging station FOEN, 2018) lead to the disconnection of the river water intakes from the pumps at both river measurement locations. The pump from the downstream location (M2) was also damaged and disconnected until the end of the experiment. After undergoing maintenance, the upstream river water intake (M1) was restored to normal operation on day 38 until the end of the injection period (day 41).

3.3.2. Efficiency of the system

We used the correlation between the discharge at the gauging station of Eggiwil and the discharge at the field site (obtained by gauging tests) used for the model of Schilling et al. (2017) to calculate the discharge at our field site. We could then calculate the efficiency (ϵ, Eq. (2)) of our injection setup. Interestingly, ϵ varies during the experiment, as it changes according to the river discharge. When the discharge exceeds 8 m^3/s, the efficiency ranges between 75% and 100%. However, for lower discharges, we observe a linear relation, with efficiency levels ranging from 40% to 80% for a discharge of 5 m^3/s, and of approximately 20% for a discharge of 2 m^3/s. This relation may be explained by stronger gas exchange between the river water and atmosphere during low discharge, i.e. when the river depth is lower. For more details, a plot relating the efficiency of the system with the river discharge is available in Appendix B.

In total, we injected the entire volume of the three 30-liter He gas tanks (18 m^3). However, the total injected volume by diffusion (obtained by integrating the injection rate $I_{\mathrm{He,tot}}$ over time) is 11.6 m^3. Therefore approximately one-third of the He used in this experiment was lost through leaks.

3.3.3. Concentrations in groundwater

Fig. 5 shows the dissolved He concentrations in the production well, being monitored for more than two months. The pumping rate of the production well was constant at circa 3700 l/min for the entire experiment. On average, the gas injection in the Emme caused an increase in concentrations of approximately 40% above background level of the well. This clearly indicates that at least part of the pumped groundwater consisted of recently infiltrated river water enriched in He. Again, the concentrations of the other gases (O_2, N_2, and Ar) remained constant during the entire experiment and a figure comparing the concentrations is available in Appendix C. The two first injection periods led to a significant increase in He concentrations, plateauing from approximately day 22. The effects of changes in He injection rate are observed at the production well with a delay of 1.5 – 2 days. This

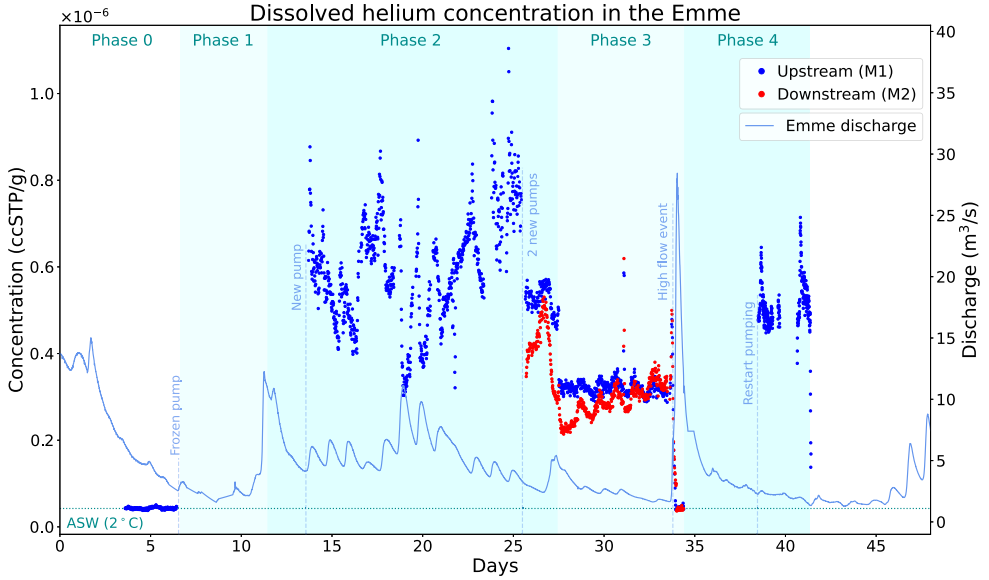

Fig. 4. Measured dissolved He concentrations in the Emme river. The different shades of blue indicate the different phases with distinct injection pressures in the silicone tubing. The discharge is measured 5 km upstream of our study site (Eggiwil gauging station). The horizontal dashed blue line is the dissolved He concentration of ASW calculated for 2 °C (the mean temperature during our experiment) and the dashed vertical lines represent significant events during the experiment (see text for details). (For interpretation of the references to color in this figure legend, the reader is referred to the web version of this article.)

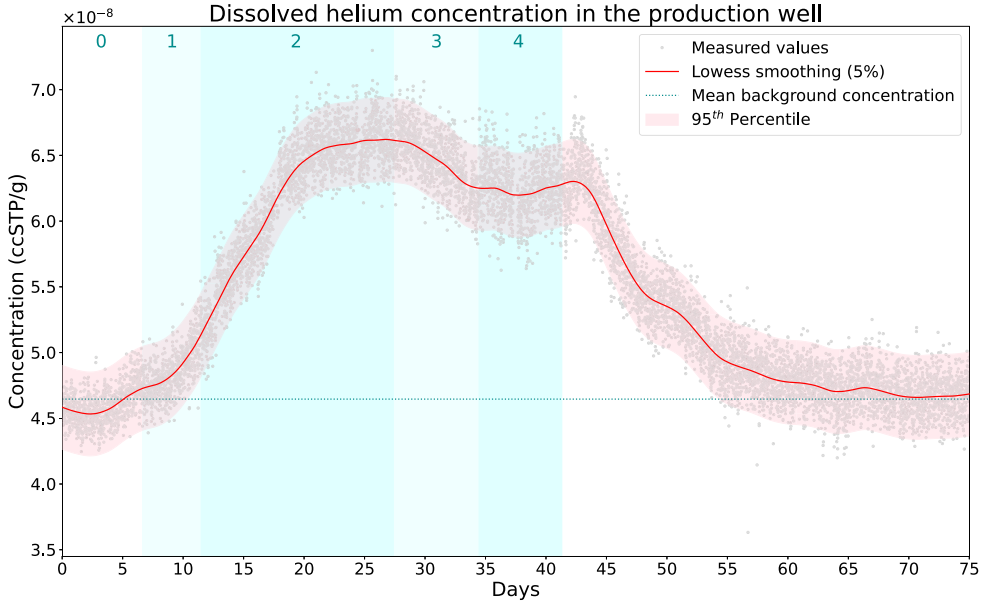

Fig. 5. Dissolved He concentration of groundwater in the drinking water production well. This figure also shows the phases with the different injection pressures (0 to 4, see Table 1). The dissolved He concentration in the groundwater starts to vary 1.5–2 days after applying change in the injection pressures in the river.

delay is especially noted when the He injection was reduce/stopped after the injection phases 2 and 4. Finally, dissolved He concentrations returned to background levels circa 20 days after the end of the He injection.

From this result, we can estimate the volume of injected He that arrived in the production well by multiplying the measured excess He concentration with the pumping rate of the production well (3700 l/min). This volume is 3200 ccSTP, equivalent to only 0.03% of the total amount of He injected by diffusion in the experiment. A simple linear binary mixing model between the river water concentration and the regional groundwater component enables us to also estimate the fraction of pumped water in the production well originating from the river: 5%–7%. For this calculation, we used the background concentration of piezometers P1 and P6 as the regional groundwater end-member, as they do not get a significant fraction of freshly infiltrating river water (see paragraph below).

Dissolved He concentrations in the six targeted piezometers are shown in Fig. 6. The different injection phases as well as the He concentrations in the production well are shown for comparison. The monitoring starts only during the second injection period as the miniRUEDIs were used for monitoring the river and the production well. Piezometers P2 and P3 both react strongly and rapidly to concentration variations in the river (over 200% increase above background). Thus, a significant part of the groundwater at these locations consists of recently infiltrated river water. Groundwater from piezometer P5 also reflects the concentration changes in the river but in a more dampened manner, indicating longer travel times and more dispersion. Interestingly, the measured peak concentration in piezometer P5 (100%

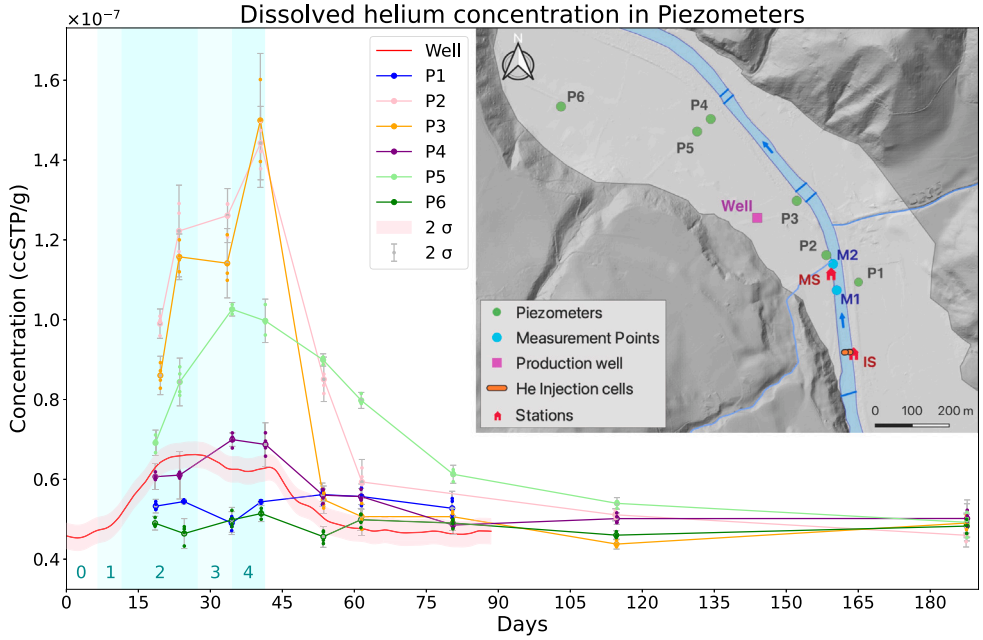

Fig. 6. Dissolved He concentration of groundwater pumped in the well and six piezometers.

increase) is much larger than in piezometer P4 (30% increase), despite P4 being closer to the river. This reflects the spatial heterogeneity of the aquifer properties at the study site, and suggests the existence of preferential flow paths, i.e. P5 intersects a preferential flow path whereas P4 lies in a low flow region. The intensity of the concentration increase in piezometer P4 is similar to that in the production well, indicating for both sampling locations that regional groundwater significantly adds to the abstracted groundwater. Finally, He concentrations remain stable at piezometers P1 and P6 for the duration the experiment, indicating little to no influence from recently infiltrated river water. Again, we compared the variations in He concentration with those of other gases to confirm that these variations were a consequence of the injection into the river.

4. Discussion

4.1. Advantage of diffusive injection

The results demonstrate the efficiency of our diffusive injection setup in rivers with highly variable discharge. This experiment required only 18 m^3 STP of He (or three 30-liter He tanks pressurized to 200 bar), leaks included, to adequately supersaturate river water by about one order of magnitude continuously for a period of over one month. As mentioned before, the setup is suitable for other gases, which can reduce or increase the final costs. Indeed, the diffusion cells could be used with other gases to which silicone is even more permeable, such as propane (C_3H_8), Ar, Ne, Kr or Xe (Barrer and Chio, 1965; Zhang and Cloud, 2006). With gases such as krypton or xenon, the injection setup could be simplified (e.g. lower number of diffusion cells and/or lowered injection pressures), as silicone rubber is respectively circa 5 and 10 times more permeable to them than to He (Barrer and Chio, 1965).

To evaluate the potential advantage of using a diffusive system for gas tracers injection into water, we compare our results to a bubbling He injection experiment that we conducted at the same river three months earlier (Blanc et al., 2021). We reached a much higher excess of dissolved He concentration (2 orders of magnitude higher than ASW) but at much smaller average river discharge of 0.4 m^3/s. The bubbling injection system was less efficient (less than 0.5%), and required 60 m^3 STP of He for a total duration of approximately 20 h. Therefore, conducting a similar 35-day experiment with this bubbling method would require approximately 15 times more gas (for equivalent river discharge and supersaturation), which is financially and logistically prohibitive. To summarize the comparison, over-saturating He by one order of magnitude compared to ASW in a 1 m^3/s discharge river for one day requires approximately 2.25 m^3STP He when applying bubbling, but only 0.15 m^3STP He when applying diffusion.

4.2. Advantage of coupling our setup with a miniRUEDI

Our results also show the potential of using noble gases to trace river water infiltration into groundwater. We compare our experiment with Clark (2020), who injected SF_6 into a river by bubbling and by diffusion and analyzed SF_6 in surrounding piezometers by gas chromatography, and thus only few temporally resolved data could be obtained. Only the gas-tagged infiltrated river water after the bubbling injection could be identified. For the diffusing injection, the authors explained the absence of SF_6 in GW by gas loss during infiltration through unsaturated pathways in the vadose zone. Perhaps increasing the length of silicone tubing to achieve a more substantial level of supersaturation might have enabled the detection of the injected gas in the groundwater. Combining our injection system with the recent development of portable mass spectrometers significantly simplifies the execution of such experiments, and results in denser time series data.

This high time resolution continuous data can readily be interpreted with simple binary mixing and lumped parameter models to determine GW transit time distributions and the fraction of recently infiltrated SW in the abstracted groundwater. Both continuous and punctual measurements of dissolved gas concentrations as carried out during our experiment may also provide valuable observations for the calibration of physically-based hydrogeological models, e.g. guiding decision for the sustainable management of drinking water resources.

4.3. Considerations for field application

The time series data for Emme water is not complete and the missing data was a result of applying our method under harsh environmental conditions, such as freezing temperatures and high flow conditions. Nevertheless, these data gaps do not compromise the outcomes of our experiment. There is potential for improvement by using more robust

pumps for such prolonged pumping, thereby avoiding data gaps and the need for additional fieldwork to replace pumps. However, such gaps in the time series of river He could be filled by estimating He concentrations from river discharge and He injection rate (see $C_{He,calc}$ in Eq. (2), section Section 3.2). Such estimation could even replace the continuous He measurement in the river if we have a good control of the injection parameters, i.e if we precisely know the injections pressures and system efficiency over the duration of the experiment.

The apparent injection efficiency of our setup declines as river discharge decreases (see Section 3.3.2 and Appendix B). As mentioned before, this is probably attributed to an increased rate of gas exchange between river water and the atmosphere for lower river discharge (our measurements at M1 and M2 confirmed that degassing occurred). This process becomes less significant for discharges exceeding 8 m^3/s, as the injection efficiency reaches a plateau and varies between 80% and 100%. This is similar to the efficiency of diffusion injection of up to 100% reported elsewhere (Benson et al., 2014; Clark, 2020). The fact that it does not stabilize at 100% may be caused by the heterogeneity of dissolved He concentrations in the river: the injected He is not perfectly mixed laterally in the river water, and the sampled water may come from a portion of the river where dissolved He concentrations are lower. In fact, we measured some degree of heterogeneity in the spatial distribution of dissolved He concentrations prior to the definitive selection of monitoring locations M1 and M2. The degree of lateral mixing of dissolved gas in river water depends on the location of the diffusion cells in relation to river morphology. This heterogeneity, likely varying as a function of river discharge, could not be accounted for during the injection experiment and could have led to some measurements not representative of the mean dissolved He concentrations in river water. This heterogeneity effect may also play a role for smaller discharges. Additionally, the discharge used to calculate theoretical He concentrations at the injection point (Q_{Emme} in Eq. (2)) might be underestimated, especially for low discharge, leading to an overestimated theoretical He concentrations ($C_{He,calc}$) and thus lower estimated efficiencies.

Our injection system is currently optimized for low- to medium-discharge rivers (up to approximately 50 m^3/s, contingent upon the specific river geometry), as it is usually easier to safely install the injection material. However, the discharge should not be too low as excessively shallow water depth may enhance the gas exchange velocity, and thus degassing. The installation is also feasible in rivers with highly variable discharge if it takes place during low flow, however sudden high discharge might damage the injection material as was the case during our experiment. Finally, our setup becomes very difficult to use in rivers with very high discharge (e.g. several hundred m^3/s), because the installation of the injection cells on the riverbed would be logistically challenging, even if theoretically possible with high financial means.

4.4. Possible enhancements and modifications

For future experiments, enhanced lateral mixing could be achieved by injecting the gas tracer further upstream so that river water is more properly mixed when it reaches suspected infiltration zones, or by injecting the gas, if possible, over the entire width of the river. If the river infiltration is suspected over a longer river section, or if weirs are in place, degassing may be important to consider. This can be achieved by measuring the dissolved gas concentration at multiple points along the river section. The outcomes of these measurements may hold significant value for numerical models since the input concentration of the SW–GW system will decrease as we move farther from the injection point.

A great advantage of our setup resides in the possibility of easily changing the injection tubes in case of damage, extending the possible duration of tracer injection experiments. This only requires to opening one cap and can be done while letting the 3-inch tubes on the riverbed. Additional sets can be prepared and kept in the field as spare material. The risk of material damage significantly increases during high-flow events, which can however often be predicted from weather forecasts. Removing the injection cells from the river before such events would prolong its lifespan. Furthermore, eliminating the leaks that constraint the current design of our diffusive injection setup will additionally improve the developed technique. This may be achieved for example by using PVC tubing with narrower screening as casing to avoid the penetration of particles big enough to perforate the silicone tubing.

Finally, using different gases could reduce the costs, but also be more efficient if more soluble in water. Moreover, injecting different gases in different stream locations can facilitate the tagging of distinct river sections, offering enhanced insights into the dynamics of the SW–GW system.

5. Conclusion

We have developed a simple and robust diffusive setup to inject high quantities of different tracer gases into medium-discharge rivers. This setup was used to inject He as an artificial tracer in a river with highly variable discharge to study SW infiltration into an alluvial aquifer. The method allowed for the enrichment He in river water by one order of magnitude compared to natural concentrations for a period of over one month, whilst reaching an injection efficiency of 85% - over two orders of magnitudes higher than commonly used bubbling methods. The developed injection system thus complements existing tracer methods, and is especially suited if significant contrasts in tracer concentrations between SW and GW do not exist or cannot be induced for sufficiently long periods. Although diffused gas injection was used before, our technique widens the scope of the diffusion method by increasing its application on larger spatial scales and for longer observational periods, which opens the method to a wide range of possible applications.

CRediT authorship contribution statement

Théo Blanc: Conceptualization, Data curation, Formal analysis, Investigation, Methodology, Project administration, Visualization, Writing – original draft, Writing – review & editing. **Morgan Peel:** Conceptualization, Data curation, Formal analysis, Investigation, Methodology, Project administration, Supervision, Validation, Writing – review & editing. **Matthias S. Brennwald:** Methodology, Resources, Software, Supervision, Validation, Writing – review & editing. **Rolf Kipfer:** Conceptualization, Supervision, Validation, Writing – review & editing. **Philip Brunner:** Conceptualization, Funding acquisition, Project administration, Resources, Supervision, Validation, Writing – review & editing.

Declaration of competing interest

The authors declare that they have no known competing financial interests or personal relationships that could have appeared to influence the work reported in this paper.

Data availability

Data will be made available on request.

Acknowledgments

The authors thank Laurent Marguet and Roberto Costa for their expertise and help on the field. They also thank the Wasserverbund Region Bern (WVRB) for allowing us to conduct this experiment in their well-field site, and Philip Waldmann for his availability on the field site. We greatfully acknowledge support from the Swiss Nation Science Foundation, grant number 200021_179017.

Appendix A. Emme: Comparison gas concentrations

See Fig. A.7

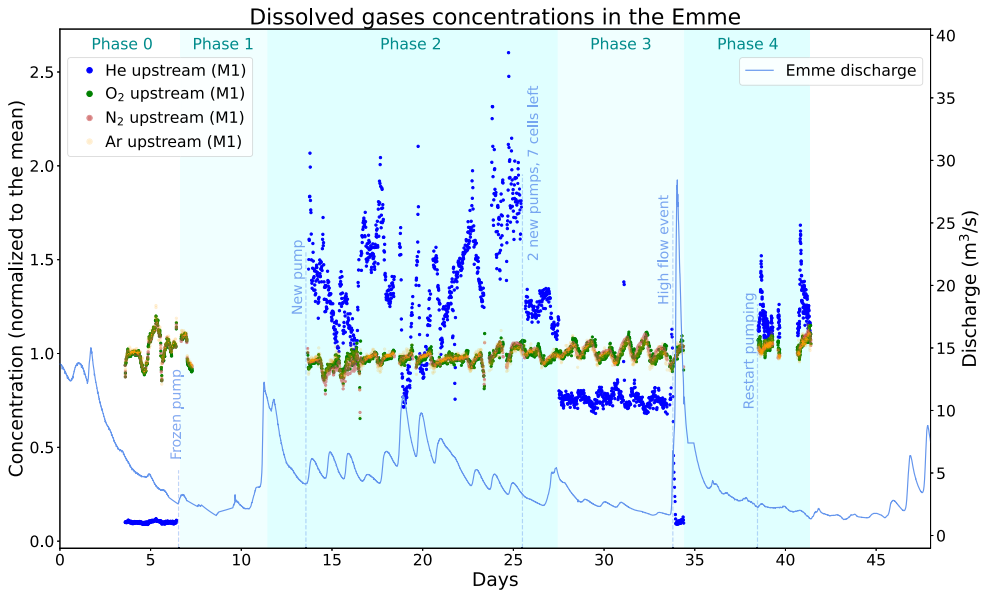

Fig. A.7. Concentrations of different gases in the river. For comparison purposes, the concentrations are relative to their means. This figure shows that the variations of the dissolved He concentration were caused by the injection of He into the river, as the concentrations of the other gases remained relatively stable.

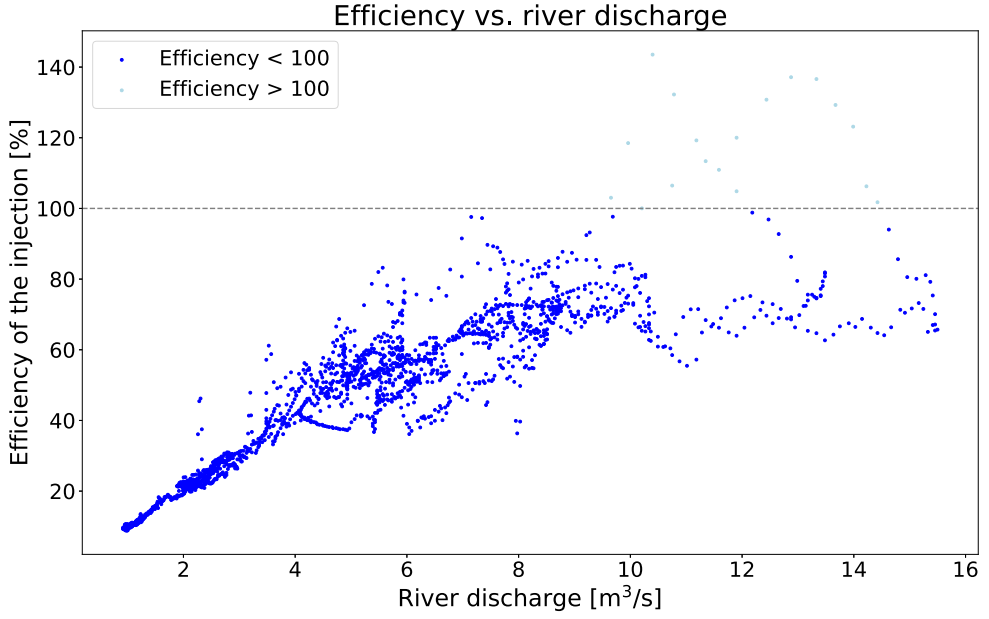

Fig. B.8. Relation between the efficiency of the injection and the river discharge. We noticed a linear relation for discharges under 8 m^3/s and a plateau for discharges above 8 m^3/s. The efficiency exceeds 100% during a rapid rise in river discharge due to inertia in our measurement system. This occurs because the measured concentrations are obtained from river water pumped prior to the significant increase in discharge, while the theoretical helium concentrations are already calculated considering the elevated discharge ($C_{He,meas}$ is higher than $C_{He,calc}$ in Eq. (2)). The measured concentrations used to calculate the efficiency are those measured at M1.

Appendix B. Injection efficiency

See Fig. B.8

Appendix C. Production well: Comparison gas concentrations

See Fig. C.9

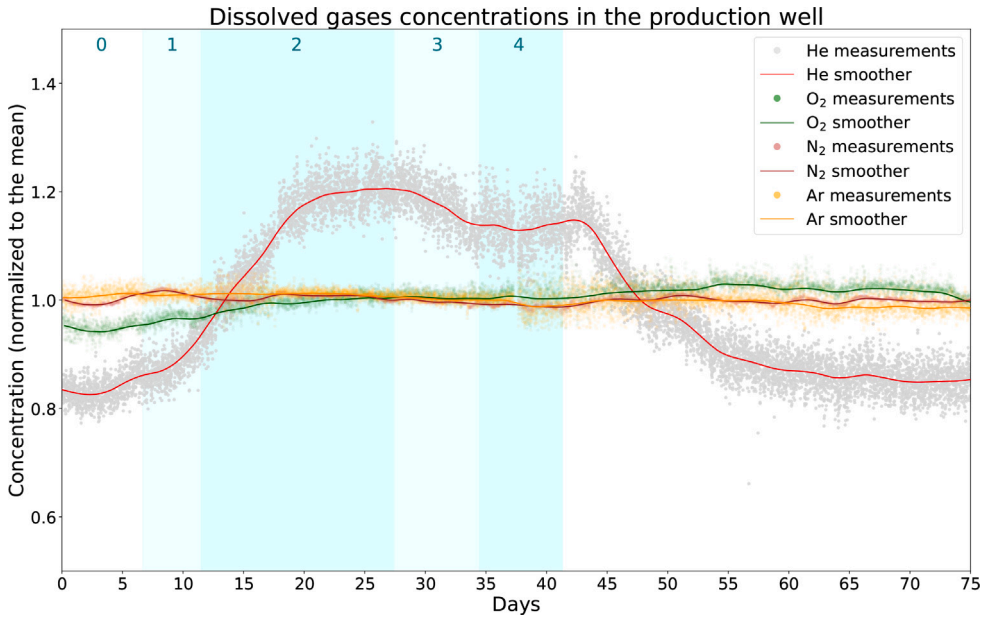

Fig. C.9. Concentrations of different gases in the production well. For comparison purposes, the concentrations are relative to their means. This figure shows that the variations of the dissolved He concentration were caused by the arrival of infiltrated river water (with excess He) in the well. The concentrations of the other gases remained relatively stable.

References

Anderson, M.P., 2005. Heat as a ground water tracer. Groundwater 43 (6), 951–968.

Barrer, R., Chio, H., 1965. Solution and diffusion of gases and vapors in silicone rubber membranes. J. Polym. Sci. C 10 (1), 111–138.

Barthel, R., Banzhaf, S., 2016. Groundwater and surface water interaction at the regional-scale–a review with focus on regional integrated models. Water Resour. Manag. 30 (1), 1–32.

Benson, A., Zane, M., Becker, T., Visser, A., Uriostegui, S., DeRubeis, E., Moran, J., Esser, B., Clark, J., 2014. Quantifying reaeration rates in alpine streams using deliberate gas tracer experiments. Water 6 (4), 1013–1027.

Blanc, T., Peel, M., Brennwald, M.S., Kipfer, R., Brunner, P., 2021. Use of helium as an artificial tracer to study surface water/groundwater exchange. In: EGU General Assembly Conference Abstracts. pp. EGU21–9005.

Boano, F., Harvey, J.W., Marion, A., Packman, A.I., Revelli, R., Ridolfi, L., Wörman, A., 2014. Hyporheic flow and transport processes: Mechanisms, models, and biogeochemical implications. Rev. Geophys. 52 (4), 603–679.

Brennwald, M., Peel, M., Blanc, T., Tomonaga, Y., Kipfer, R., Brunner, P., Hunkeler, D., 2022. New experimental tools to use noble gases as artificial tracers for groundwater flow. Front. Water 4, 925294.

Brennwald, M.S., Schmidt, M., Oser, J., Kipfer, R., 2016. A portable and autonomous mass spectrometric system for on-site environmental gas analysis. Environ. Sci. Technol. 50 (24), 13455–13463, PMID: 27993051.

Brunner, P., Therrien, R., Renard, P., Simmons, C.T., Franssen, H.-J.H., 2017. Advances in understanding river-groundwater interactions. Rev. Geophys. 55 (3), 818–854.

Cecil, L.D., Green, J.R., 2000. Radon-222. In: Environmental Tracers in Subsurface Hydrology. Springer US, pp. 175–194.

Chatton, E., Labasque, T., de La Bernardie, J., Guihéneuf, N., Bour, O., Aquilina, L., 2017. Field continuous measurement of dissolved gases with a CF-MIMS: Applications to the physics and biogeochemistry of groundwater flow. Environ. Sci. Technol. 51 (2), 846–854.

Cirpka, O.A., Fienen, M.N., Hofer, M., Hoehn, E., Tessarini, A., Kipfer, R., Kitanidis, P.K., 2007. Analyzing bank filtration by deconvoluting time series of electric conductivity. Ground Water 45 (3), 318–328.

Cirpka, O., Reichert, P., Wanner, O., Mueller, S.R., Schwarzenbach, R.P., 1993. Gas exchange at river cascades: field experiments and model calculations. Environ. Sci. Technol. 27 (10), 2086–2097.

Clark, J., 2020. Defining transport near ASR operations using sulfur hexafluoride gas tracer experiments. In: Management of Aquifer Recharge for Sustainability. CRC Press, pp. 257–260.

Clark, J.F., Hudson, G.B., Avisar, D., 2005. Gas transport below artificial recharge ponds: Insights from dissolved noble gases and a dual gas (SF6 and 3He) tracer experiment. Environ. Sci. Technol. 39 (11), 3939–3945.

Cook, P.G., Lamontagne, S., Berhane, D., Clark, J.F., 2006. Quantifying groundwater discharge to Cockburn River, southeastern Australia, using dissolved gas tracers ^{222}Rn and SF_6: Groundwater discharge to the cockburn. Water Resour. Res. 42 (10).

Coplen, T.B., Herczeg, A.L., Barnes, C., 2000. Isotope engineering - using stable isotopes of the water molecule to solve practical problems. In: Environmental Tracers in Subsurface Hydrology. Springer, pp. 79–110.

Davis, S.N., Campbell, D.J., Bentley, H.W., Flynn, T.J., 1985. Introduction to ground-water tracers. Final report, September 1982-December 1984.

Davis, S.N., Thompson, G.M., Bentley, H.W., Stiles, G., 1980. Ground-water tracers—A short review. Groundwater 18 (1), 14–23.

Daynes, H.A., 1920. The process of diffusion through a rubber membrane. Proc. R. Soc. Lond. A 97 (685), 286–307.

FOEN, 2018. Federal office of the environment (BAFU). Hydrological data and forecast. url: https://www.hydrodaten.admin.ch, Station 2409: Emme - Eggiwil, Heidbüel, Annual indices: discharge 2018.

Hall Jr., R.O., Madinger, H.L., 2018. Use of argon to measure gas exchange in turbulent mountain streams. Biogeosciences 15 (10), 3085–3092.

Hoehn, E., Von Gunten, H., 1989. Radon in groundwater: A tool to assess infiltration from surface waters to aquifers. Water Resour. Res. 25 (8), 1795–1803.

Käser, D., Hunkeler, D., 2016. Contribution of alluvial groundwater to the outflow of mountainous catchments. Water Resour. Res. 52 (2), 680–697.

Kipfer, R., Aeschbach-Hertig, W., Peeters, F., Stute, M., 2002. Noble gases in lakes and ground waters. Rev. Mineral. Geochem. 47 (1), 615–700.

Knapp, J.L.A., Osenbrück, K., Brennwald, M.S., Cirpka, O.A., 2019. In-situ mass spectrometry improves the estimation of stream reaeration from gas-tracer tests. Sci. Total Environ. 655, 1062–1070.

Knapp, J.L.A., Osenbrück, K., Cirpka, O.A., 2015. Impact of non-idealities in gas-tracer tests on the estimation of reaeration, respiration, and photosynthesis rates in streams. Water Res. 83, 205–216.

Lamontagne, S., Cook, P.G., 2007. Estimation of hyporheic water residence time in situ using 222Rn disequilibrium. Limnol. Oceanogr.: Methods 5 (11), 407–416.

Lin, A.Y.-C., Debroux, J.-F., Cunningham, J.A., Reinhard, M., 2003. Comparison of rhodamine WT and bromide in the determination of hydraulic characteristics of constructed wetlands. Ecol. Eng. 20 (1), 75–88.

Mächler, L., Brennwald, M.S., Kipfer, R., 2012. Membrane inlet mass spectrometer for the quasi-continuous on-site analysis of dissolved gases in groundwater. Environ. Sci. Technol. 46 (15), 8288–8296.

MeteoSwiss, 2021. Federal office of meteorology and climatology, measurement values. https://www.meteoswiss.admin.ch/home/measurement-values.html.

Poff, N.L., Zimmerman, J.K., 2010. Ecological responses to altered flow regimes: a literature review to inform the science and management of environmental flows. Freshwater Biol. 55 (1), 194–205.

Popp, A.L., Pardo-Álvarez, Á., Schilling, O.S., Scheidegger, A., Musy, S., Peel, M., Brunner, P., Purtschert, R., Hunkeler, D., Kipfer, R., 2021. A framework for untangling transient groundwater mixing and travel times. Water Resour. Res. 57 (4), e2020WR028362.

Schilling, O.S., Cook, P.G., Brunner, P., 2019. Beyond classical observations in hydrogeology: The advantages of including exchange flux, temperature, tracer concentration, residence time, and soil moisture observations in groundwater model calibration. Rev. Geophys. 57 (1), 146–182.

Schilling, O.S., Gerber, C., Partington, D.J., Purtschert, R., Brennwald, M.S., Kipfer, R., Hunkeler, D., Brunner, P., 2017. Advancing physically-based flow simulations of alluvial systems through atmospheric noble gases and the novel ^{37}Ar tracer method. Water Resour. Res. 53 (12), 10465–10490.

Stute, M., Deák, J., Révész, K., Böhlke, J., Deseö, É., Weppernig, R., Schlosser, P., 1997. Tritium/3He dating of river infiltration: An example from the Danube in the Szigetkoez area, Hungary. Groundwater 35 (5), 905–911.

Swisstopo, 2021. Federal office of topography. https://www.swisstopo.admin.ch/de/geodata/maps/smr/smr25.html.

Vautier, C., Abhervé, R., Labasque, T., Laverman, A.M., Guillou, A., Chatton, E., Dupont, P., Aquilina, L., de Dreuzy, J.-R., 2020. Mapping gas exchanges in headwater streams with membrane inlet mass spectrometry. J. Hydrol. 581, 124398.

Würsten, M., 1991. GWB–hydrogeologische untersuchungen aeschau: Schlussbericht. Technical Report, Zurich: Geotechnisches Institut.

Zhang, H., Cloud, A., 2006. The permeability characteristics of silicone rubber. Glob. Adv. Mater. Process Eng. 72–75.